Poly(norbornenyl azlactone) as a versatile platform for sequential double click postpolymerization modification

Francesca François, Clémence Nicolas, Gwénaël Forcher, Laurent Fontaine, V. Montembault

Poly(norbornenyl azlactone) as a versatile platform for sequential double click postpolymerization modification

Francesca François, Clémence Nicolas, Gwénaël Forcher, Laurent Fontaine, Véronique Montembault**

Institut des Molécules et Matériaux du Mans (IMMM) - UMR 6283 CNRS, Le Mans Université, Avenue Olivier Messiaen, 72085 Le Mans Cedex 9, France

* Address correspondence to:
Laurent Fontaine: laurent.fontaine@univ-lemans.fr; Véronique Montembault: veronique.montembault@univ-lemans.fr

Keywords: ring-opening metathesis polymerization (ROMP), Grubbs 3rd generation catalyst, azlactone-containing norbornene monomer, click chemistry, postpolymerization modification.

Abstract

Ring-opening metathesis polymerization (ROMP) of a heterofunctional azlactone-based monomer, namely norbornenyl azlactone (NBAzl), is reported for the first time using third generation ruthenium-based catalyst (**G3'**). It is demonstrated that ROMP of the mixture of stereoisomers of NBAzl obtained by Diels-Alder reaction between 2-vinyl-4,4-dimethyl-5-oxazolone (vinyl azlactone, VDM) and cyclopentadiene leads to well-defined polymers ($\overline{M_{n,\,SEC}}$ up to 52 500 g mol^{-1}, $Đ$ < 1.37). The resulting polymers easily undergo click postpolymerization modification by aminolysis of the azlactone groups using amine nucleophiles. By using azido oligoethylene glycol amine, ROMP polymers having azido side-chains capable of alkyne azide click modification are prepared, that are not attainable by direct ROMP of azido-functionalized monomers. The successful clicking to the so-obtained azido-functional ROMP polymer was demonstrated by copper-catalyzed alkyne–azide cycloaddition (CuAAC) with alkyne-functionalized fluorescein. The reported versatile methodology produces with complete atom economy a platform for new functional polymer libraries, including polymer materials with potential medical and biological applications.

1. Introduction

Postpolymerization modification (PPM), also known as polymer analogous reaction, is an attractive alternative to polymerization of functional monomers to obtain useful polymer-based materials with specific properties and topologies [1-7]. By chemically modifying a polymeric precursor after the polymer has been prepared, PPM allows for the synthesis of a diverse library of functional polymers from a single polymer precursor and avoids possible adverse side reactions that may occur with certain functional groups during polymerization.

Nowadays, controlled/living polymerization techniques allow the synthesis of polymers with precise control over molecular weight, composition, and architecture. Well-defined polymers can thus be produced using heterofunctional monomers, *i.e.*, monomers having chemical handles that are inert towards the polymerization conditions but which can be quantitatively converted in a subsequent PPM step into a broad range of other functional groups.

Because the activated ester-amine chemistry has many characteristics of conventional click chemistries, featuring metal free and mild reaction conditions, the nucleophilic substitution of polymeric active esters such as *N*-hydroxysuccinimide (NHS) and pentafluorophenyl (PFP) esters with amine derivatives has become the most common form of PPM [8,9]. However, these activated ester groups suffer from a limited hydrolytic stability and from the toxicity of the leaving group that is released during the PPM step which is not atom-efficient or economical [10].

To circumvent the drawbacks associated with the use of activated esters, the azlactone (or oxazolone) functionality has emerged as a powerful chemical handle because of its high reactivity towards amine nucleophiles without generating by-products or requiring a catalyst [11-13]. The aminolysis reaction takes place with complete atom economy and can be conducted in a broad range of organic solvents as well as in aqueous solution at room temperature, exhibiting the advantages of conventional click-type reactions [13-15].

Moreover, unlike emerging catalyzed approaches for the direct PPM conversion of esters to amides [16-19], the azlactone group reacts efficiently and selectively with amines without requiring the presence of a catalyst. PPM of (co)polymers derived from 2-vinyl-4,4-dimethyl azlactone (VDM) has thus been widely explored for various applications [20-36], including bioconjugation [14,37-42].

Among the different controlled/living polymerization techniques, ring-opening metathesis polymerization (ROMP) of strained cyclic alkenes such as norbornenes has become a versatile and widely used method to synthesize functional polymers in a controlled fashion [43,44]. Thanks to the development of highly active ruthenium-based initiators, ROMP offers an attractive route for the preparation of synthetic polymers displaying a diverse array of functionalities with precise control over molecular weight and composition while release of ring strain provides the driving force for high conversion in these systems [44-48]. In addition, polymers generated by ROMP feature a double bond in the backbone, which can be used for further functionalization. Among the reactive monomers that can be used in ROMP, a number of norbornene-derived monomers bearing activated esters such as NHS or PFP esters have been employed in PPM reactions to generate various polymer-based bioconjugates [8,47-51].

Our group has previously been reporting the ROMP of norbornenyl azlactone (2-(norborn-2-en-5-yl)-4,4-dimethyl-5-oxazolone**, NBAzl** in Scheme 1) [52,53], an azlactone-based norbornene derivative that was originally described for photoinitiated thiol-ene reactions [54]. In our first report, ROMP of **NBAzl** was conducted in the presence of Ru-based initiators (first and second generation Grubbs' catalysts) and the subsequent PPM using methyl glycinate, aqueous base or *N,N*-diethylamine gave the corresponding functionalized polymers with quantitative yields. However, it was found that ROMP of the mixture of stereoisomers could not be achieved efficiently, the *endo* isomer being much less reactive than its *exo* counterpart, which requires the prior separation of the stereoisomers from the *endo/exo* mixture. In addition, the corresponding polymers had high dispersities, a result which can be attributed to the low reactivity of the catalyst, slow rates of initiation compared to propagation, and to competitive chain transfer reactions [46,55]. Given the availability of the highly efficient third generation Ru-based initiator **G3'** (Scheme 1) [55], we decided to re-investigate the ROMP of the *endo/exo* mixture of **NBAzl**. We therefore report herein the synthesis of well-defined poly(norbornenyl azlactone) (**PNBAzl**) using **G3'** catalyst and subsequent efficient PPM using amine nucleophiles. By using an azido-functionalized nucleophile we also demonstrate that subsequent click copper-catalyzed alkyne–azide cycloaddition (CuAAC) can be efficiently conducted on the resulting polymers having pendant azido groups. Because azides (and alkynes) are not compatible with ruthenium-based initiators [48,56-59], the reported synthetic methodology provides unique access to ROMP polymers having azido pendant groups capable of alkyne-azide click modification. This sequential double click PPM strategy makes **PNBAzl** a unique platform for designing new functional polymers.

2. Experimental

2.1. General Characterization

Nuclear magnetic resonance (NMR) spectra were recorded on a Bruker AC-400 spectrometer operating at 400.16 MHz for ^{1}H NMR and 100.62 MHz for ^{13}C NMR. The chemical shifts are reported in parts per million (ppm) relative to deuterated solvent resonances. The average molar masses (number-average molar mass $\overline{M_n}$, weight-average molar mass $\overline{M_w}$) and dispersity ($Đ = \overline{M_w}/\overline{M_n}$) values of poly(norbornenyl azlactone)s (**PNBAzl**) and **PNBAzl** modified with 11-azido-3,6,9-trioxaundecan-1-amine (**m-PNBAzl-N$_3$**) of number-average degree of polymerization ($\overline{DP_n}$) of 50 were measured by size exclusion chromatography (SEC) using tetrahydrofuran (THF) as an eluent, and carried out using a system equipped with a Waters 2707 autosampler, with a guard column (Waters, Styragel, 20 µm Guard column, 30 x 4.6 mm) followed by two columns (Waters, 2 Styragel THF HR2+HR4, 300 x 7.8 mm) and with a Waters RI-2414 detector. The instrument operated at a flow rate of 1.0 mL.min^{-1} at 35°C and was calibrated with narrow linear polystyrene (PS) standards ranging in molar mass from 580 g.mol^{-1} to 483 000 g.mol^{-1}. The average molar masses ($\overline{M_n}$, $\overline{M_w}$) and $Đ$ values of **PNBAzl** modified with 1-aminopropan-2-ol (**m-PNBAzl-OH**), **PNBAzl** modified with 1-aminopropan-2-ol and 11-azido-3,6,9-trioxaundecan-1-amine at a feed molar ratio of 90:10 (**(m-PNBAzl-OH)$_{90}$-*co*-(m-PNBAzl-N$_3$)$_{10}$**) of DP_n = 100, and fluorescein-carrying modified **PNBAzl** (**(m-PNBAzl-OH)$_{90}$-*co*-(m-PNBAzl-fluorescein)$_{10}$**) were measured by gel permeation chromatography (GPC) using *N,N*-dimethylformamide (DMF) with LiBr at 1g·L^{-1} as an eluent and carried out using a system equipped with a guard column (Polymer Laboratories, PL gel 5 µm) followed by two columns (2 Phenomenex Phenogel 5 µm columns, 500 Å and 10^4 Å porosity) with a Shimadzu RID-10A differential refractometer (DRI) and a Shimadzu APD-20A UV detector operating at 633 and 285 nm, respectively. The instrument operated at a flow rate of 1.0 mL·min^{-1} at 50 °C and was calibrated with narrow linear poly(methyl methacrylate) (PMMA) standards ranging in molecular weight from 904 to 304,000 g·mol^{-1}. Attenuated Total Reflectance (ATR) Fourier Transform Infra-Red (FT-IR) spectra were obtained using a Nicolet avatar 370 DTGS system. Spectra were obtained at regular time intervals in the MIR region of 4000-500 cm^{-1} at a resolution of 4 cm^{-1} (640 scans) and analyzed using OPUS software.

2.2. Materials

All the reagents used in this study were purchased from Sigma-Aldrich, unless otherwise noted. 1-Aminopropan-2-ol (93%), 11-azido-3,6,9-trioxaundecan-1-amine (90%), copper(I) bromide (Cu(I)Br, 99,99%), deuterated chloroform ($CDCl_3$, 99.8% D, 0.03% TMS, Euriso-top), deuterated dimethyl sulfoxide (DMSO-d_6, 99.8% D, Euriso-top), dichloroethane (DCE, 99.8%), *N,N*-dimethylformamide (DMF, 99.8%), dimethyl sulfoxide (DMSO, 99.8%), ethyl vinyl ether (99%, Acros), fluorescein alkyne (FAM-alkyne; 5-isomer, ≥95%, Lumiprobe), *n*-hexane (95%, Biosolve), neutral alumina, *N,N,N',N',N''*-pentamethyldiethylenetriamine (PMDETA, 99%), and tetrahydrofuran (99%) were used as received. Nanopure water was obtained from a reverse-osmosis purification system and had a conductivity of 18.2 MΩ cm at 25 °C. Dialysis membrane tubing with a molar mass cutoff (MWCO) of 3.5 kDa was purchased from Spectrum Laboratories, Inc. (Rancho Dominguez, CA, USA) and soaked for 5 min in nanopure water at room temperature before use. (1,3-Bis-(2,4,6-trimethylphenyl)-2-imidazolidinylidene)dichloro- (phenylmethylene)bis(pyridine)ruthenium [60] (**G3′**) and norbornenyl azlactone [52] (**NBAzl**) were synthesized according to literature procedures.

2.3. General procedure for ROMP

In a typical experiment, a dry Schlenk tube was charged with the desired quantity of **NBAzl** and a stir bar. The Schlenk tube was capped with a rubber septum and subjected to six freeze-pump-thaw cycles. The desired amount of degassed, anhydrous DCE was added via a syringe under a nitrogen atmosphere to dissolve **NBAzl** ([**NBAzl**] = 0.487 mol L^{-1}, Table S1 in SI). A stock solution of **G3'** in 1mL of degassed anhydrous DCE was prepared in a separate vial. The desired quantity of catalyst **G3'** was injected quickly into the monomer solution to initiate the polymerization (initial reaction time, t = 0). The Schlenk tube was then immersed in an oil bath preset at 70°C and was stirred under argon for 24 h. Polymerizations were quenched by adding two drops of ethyl vinyl ether. Solvent was removed under reduced pressure from the final reaction mixture. The resulting green very viscous solution was then diluted in DCE and passed through a neutral alumina column. The resulting polymer solution was precipitated into 20 mL of stirred cold *n*-hexane, filtered and dried overnight under reduced pressure.

Poly(norbornenylazlactone) (PNBAzl). Greenish plastic (79 mg, yield: 79%). $[\mathbf{NBAzl}]_0/[\mathbf{G3'}]_0$ = 100 (Table 1, run 1); conversion: 100%; $\overline{M_{n,SEC}}$ (THF) = 20 600 g.mol^{-1}; $Đ$ = 1.14. ^{1}H NMR (400 MHz, DMSO-d_6), δ (ppm): 5.44 (bs, 1nH, =CH_{trans}), 5.26 (bs, 1nH, =CH_{cis}), 3.14 (bs, 1nH, =CH-C*H*-CH), 2.90 (bs, 1nH, =CH-CH-C*H*-CN), 2.70 (bs, 1nH, =CH-C*H*-CH_2), 1.98 (bs, 2nH, =CH-CH-CH_2-CH-CN), 1.69 (bs, 2nH, (=CH-CH-CH_2-CH-CH=), 1.27 (bs, 6nH, CH_3) (Fig. 1A). ^{13}C NMR (100 MHz, DMSO-d_6), δ (ppm): 181.84 (*C*=O), 175.78 (*C*=N), 133.77 (=*C*H-CH-CH_2-CH-C=N), 129.38 (=*C*H-CH-CH), 65.12 (*C*(CH_3)$_2$), 55.03 (=CH-*C*H-CH_2-CH-C=N), 45.28 (*C*H-C=N), 45.23 (=CH-*C*H-CH), 42.54 (=CH-CH-*C*H_2-CH-CH=), 37.58 (*C*H_2-CH-C=N), 24.26 (*C*H_3). FT-IR (cm^{-1}): 2932 (ν C-H alkane), 1813 (ν C=O), 1668 (ν C=N), 1455 (δ C-H alkene), 1203 (ν O-C-O), 708 (γ C-H alkane), 653 (γ C-H alkene) (Fig. S1 in SI).

2.4. Kinetic studies

$[\mathbf{NBAzl}]_0/[\mathbf{G3'}]_0 = 100$. A typical ROMP procedure was carried out. Aliquots of reaction mixture were taken at different reaction times and polymerization was quenched by adding two drops of ethyl vinyl ether for ^{1}H NMR spectroscopy analysis. Aliquots were passed through a neutral alumina column. The solvent of aliquots was then removed under reduced pressure for further SEC measurements to determine number-average molar masses (M_n) and dispersity ($Đ$).

2.5. Postpolymerization modification of PNBAzl with 1-aminopropan-2-ol

In a typical experiment, **PNBAzl** (50 mg; 0.24 mmol in azlactone units) of $\overline{DP_n} = 100$, 1-aminopropan-2-ol (21 mg; 0.28 mmol), and $CDCl_3$ (0.5 mL) were charged to a 5 mL vial equipped with a stir bar. The mixture was bubbled with a slow stream of argon for 5 minutes and the vial was capped with a rubber septum. The solution was subsequently stirred at room temperature for 16 h and directly analyzed by ^{1}H NMR. Solvent was then removed under reduced pressure for further SEC measurements.

m-PNBAzl-OH. Brown powder (68 mg, yield: 99%). $\overline{DP_n} = 100$; conversion: 100%; $\overline{M_{n,SEC}}$ (DMF) = 26 500 g.mol^{-1}; $Đ = 1.60$ (Fig. S2 in SI). ^{1}H NMR (400 MHz, DMSO-d$_6$), δ (ppm): 7.80 (bs, 1nH, N*H*-C(CH$_3$)$_2$), 7.18 (bs, 1nH, N*H*-CH$_2$), 5.35 (bs, 1nH, =C*H*$_{trans}$), 5.21 (bs, 1nH, =C*H*$_{cis}$), 3.63 (bs, 1nH, =CH-C*H*-CH-CO-NH), 3.55 (bs, 1nH, C*H*-OH), 3.52 (bs, 1nH, =CH-C*H*-CH$_2$), 2.96 (bs, 3nH, C*H*$_2$-CH-CO-NH, C*H*-CO-NH), 2.35 (bs, 2nH, CO-NH-C*H*$_2$), 1.87 (bs, 2nH, =CH-CH-C*H*$_2$-CH-CH=), 1.29 (bs, 6nH, C(C*H*$_3$)$_2$), 1.00 (m, 3nH, CH(OH)-C*H*$_3$) (Fig. S3 in SI). ^{13}C NMR (100 MHz, DMSO-d$_6$), δ (ppm): 174.58 (*C*=O), 134.18 (=*C*H-CH-CH$_2$-CH-CO), 130.99 (=*C*H-CH-CH), 79.84 (*C*H-OH), 72.22 (*C*(CH$_3$)$_2$), 67.70 (NH-*C*H$_2$), 56.39 (=CH-*C*H-CH$_2$-CH-CO), 52.90 (=CH-*C*H-CH), 49.59 (*C*H-CO-NH), 45.67

(=CH-CH-CH_2-CH-CH=), 36.40 (CH_2-CH-CO), 21.30 (C(CH_3)$_2$), 19.41 (CH(OH)-CH_3). FT-IR (cm^{-1}): 3004 (ν O-H, ν N-H), 2970 (ν C-H alkane), 1650 (ν C=O amide), 1531 (δ N-H amide), 1454 (δ C-H alkene), 726 (γ C-H alkane), 645 (γ C-H alkene) (Fig. S4 in SI).

2.6. Postpolymerization modification of PNBAzl with 11-azido-3,6,9-trioxaundecan-1-amine.

In a typical experiment, **PNBAzl** (108 mg; 0.49 mmol in Azl units) of $\overline{DP_n}$ = 50, 11-azido-3,6,9-trioxaundecan-1-amine (126 mg; 0.54 mmol), and DCE (1 mL) were charged to a 10 mL round-bottom flask equipped with a reflux condenser and a stir bar. The mixture was bubbled with a slow stream of argon for 5 minutes. The round-bottom flask was then immersed in an oil bath preset at 50°C and was stirred under argon for 3 h. After evaporation, the resulting brown solid was then transferred to dialysis tubings and dialyzed against nanopure water for at least 3 days, followed by freeze drying to afford the final **m-PNBAzl-N_3**.

m-PNBAzl-N_3. Brown powder (192 mg, yield: 92%). $\overline{DP_n}$ = 50; conversion: 100%; $\overline{M_{n,SEC}}$ (THF) = 11 000 $g.mol^{-1}$; $Đ$ = 1.20 (Fig. S5 in SI). ^1H NMR (400 MHz, $CDCl_3$), δ (ppm): 6.92 (bs, 2nH, N*H*), 5.31 (bs, 2nH, =C*H*), 5.21 (bs, 1nH, =CH_{cis}), 3.87-3.25 (bs, 16nH, CH_2-CH_2-O and CH_2-CH_2-N_3), 3.14 (bs, 1nH, =CH-C*H*-CH-CO-NH), 2.68 (bs, 3nH, =CH-C*H*-CH_2-CH-CO-NH), 2.39 (bs, 2nH, CH_2-CO-NH), 2.39 (bs, 2nH, CH_2-CO-NH), 1.87 (bs, 2nH, =CH-CH-CH_2-CH-CH=), 1.29 (bs, 6nH, C(CH_3)$_2$), 1.00 (m, 3nH, CH(OH)-CH_3) (Fig. S6 in SI). FT-IR (cm^{-1}): 3310 (ν N-H), 2866 (ν C-H alkane), 2100 (ν N_3), 1659 (ν C=O amide), 1520 (δ N-H amide), 1451 (δ C-H alkene), 707 (γ C-H alkane), 650 (γ C-H alkene) (Fig. S7 in SI).

2.7. Postpolymerization modification of PNBAzl with 1-aminopropan-2-ol and 11-azido-3,6,9-trioxaundecan-1-amine in a 90/10 molar ratio.

In a typical experiment, **PNBAzl** (100 mg; 0.48 mmol in Azl units) of $\overline{DP_n}$ = 100, 11-azido-3,6,9-trioxaundecan-1-amine (11 mg; 50 µmol), and DCE (20 mL) were charged to a 50 mL round-bottom flask equipped with a reflux condenser and a stir bar. The mixture was bubbled with a slow stream of argon for 5 minutes. The round-bottom flask was then immersed in an oil bath preset at 50°C and was stirred under argon for 72 h. After cooling at 20 °C, 1-aminopropan-2-ol (33 mg; 0.44 mmol) was added to the reaction mixture, and the reaction was continued for 4h. After evaporation, the resulting brown solid was then transferred to dialysis tubings and dialyzed against nanopure water for at least 3 days, followed by freeze drying to afford the final **(m-PNBAzl-OH)$_{90}$-*co*-(m-PNBAzl-N$_3$)$_{10}$**.

(m-PNBAzl-OH)$_{90}$-*co*-(m-PNBAzl-N$_3$)$_{10}$. Brown powder (125 mg, yield: 87%). $\overline{DP_n}$ = 100; conversion: 100%; $\overline{M_{n,SEC}}$ (DMF) = 32 400 g.mol^{-1}; $Đ$ = 1.19 (Fig. S8 in SI). ^{1}H NMR (400 MHz, DMSO-d$_6$), δ (ppm): 6.92 (bs, 2nH, N*H*), 5.31 (bs, 1nH, =CH_{trans}), 5.21 (bs, 1nH, =CH_{cis}), 4.45 (bs, 0.9nH, O*H*), 3.86-3.25 (bs, 2.5nH, CH_2-CH_2-O and CH_2-CH_2-N$_3$, C*H*-OH), 3.20-2.60 (bs, 3nH, =CH-C*H*, C*H*-CO-NH), 2.39 (bs, 1.8nH, CH_2-NH-CO), 1.87 (bs, 4nH, =CH-CH-CH_2), 1.29 (bs, 6nH, C(CH_3)$_2$), 1.00 (m, 2.7nH, CH(OH)-CH_3) (Fig. 1B). ^{13}C NMR (100 MHz, DMSO-d$_6$), δ (ppm): 174.54 (*C*=O), 138.40-127.15 (=*C*H), 79.67 (*C*H-OH), 70.28 (*C*H$_2$-O), 69.35 (*C*H$_2$-N$_3$), 65.46 (*C*(CH$_3$)$_2$), 50.68 (NH-*C*H$_2$), 49.28 (*C*H-CO-NH), 45.93 (=CH-*C*H-*C*H), 43.80-41.45 (=CH-CH-*C*H$_2$-CH-CH=), 38.50-35.20 (*C*H$_2$-CH-CO), 27.89 (C(*C*H$_3$)$_2$), 21.35 (CH(OH)-*C*H$_3$). FT-IR (cm^{-1}): 3288 (ν N-H, ν O-H), 2929 (ν C-H alkane), 2104 (ν N$_3$), 1646 (ν C=O amide), 1528 (δ N-H amide), 1452 (δ C-H alkene), 729 (γ C-H alkane), 644 (γ C-H alkene) (Fig. S9 in SI).

2.8. Click functionalization of (m-PNBAzl-OH)$_{90}$-co-(m-PNBAzl-N$_3$)$_{10}$

For clicking alkynylated fluorescein to **(m-PNBAzl-OH)$_{90}$-*co*-(m-PNBAzl-N$_3$)$_{10}$**, azido-functionalized polymer of $\overline{DP_n}$ = 100 (1.13 μmol), alkyne FAM (10.2 μmol) and *N*,*N*,*N'*,*N'*,*N''*-pentamethyldiethylenetriamine (PMDETA; 2.9 mg, 12.2 μmol) were charged to a dry Schlenk tube along with degassed DMF (4 mL). The tube was sealed with a rubber septum and subjected to six freeze-pump-thaw cycles. This solution was then cannulated under nitrogen into another Schlenk tube, previously evacuated and filled with nitrogen, containing Cu(I)Br (0.47 mg, 3.26 μmol) and a stir bar. The resulting solution was subsequently stirred at room temperature for 24 h. The reaction mixture was passed through a short neutral alumina column before purified by a three-days dialysis against Nanopure water with MWCO 3.5 kDa and freeze drying.

(m-PNBAzl-OH)$_{90}$-*co*-(m-PNBAzl-fluorescein)$_{10}$. yellow solid (31 mg, yield: 81%). $\overline{DP_n}$ = 100; $\overline{M_{n,SEC}}$ (DMF) = 38 800 g.mol^{-1}; $Đ$ = 1.67 (Fig. S10 in SI). ^{1}H NMR (400 MHz, DMSO-d$_6$), δ (ppm): 7.90-7.02 (bs, 2.5nH, N*H*, C*H*$_{triazole}$, NH-CO-C*H*$_{Ar}$), 6.68 (s, 0.2nH, O-C*H*$_{Ar}$-OH), 6.54 (bs, 0.4nH, HO-C*H*$_{Ar}$-C*H*$_{Ar}$), 5.47-5.04 (bs, 2nH, =C*H*), 4.61-4.33 (bs, 1.3nH, O*H*, C$_{triazole}$-C*H*$_2$-NH-CO), 3.73-3.43 (bs, 2.5nH, C*H*$_2$-C*H*$_2$-O, C*H*-OH), 3.22-2.60 (bs, 3nH, =CH-C*H*, C*H*-CO-NH), 2.39 (bs, 1.8nH, C*H*$_2$-NH-CO), 2.04-1.47 (bs, 4nH, =CH-CH-C*H*$_2$), 1.30 (bs, 6nH, C(C*H*$_3$)$_2$), 0.99 (m, 2.7nH, CH(OH)-C*H*$_3$) (Fig. 1C).

3. Results and discussion

3.1. ROMP of norbornenylazlactone

Norbornenylazlactone **(NBAzl)** was prepared by a Diels-Alder cycloaddition between cyclopentadiene and 2-vinyl-4,4-dimethyl-5-oxazolone according to a literature procedure [52]. The *endo*/*exo* ratio, calculated from ^{1}H nuclear magnetic resonance (NMR) spectrum by the comparison of integrations of the signals related to the olefinic protons in *endo*-position at δ = 5.87 and 6.24 ppm (labeled c_{endo} and b_{endo}, Fig. S11 in SI) and in *exo*-position at δ = 6.16 and 6.19 ppm (labeled c_{exo} and b_{exo}, Fig. S11 in SI), was estimated at 67/33. Ring-opening metathesis polymerization (ROMP) of **NBAzl** was then conducted at 70°C in dichloroethane (DCE) using Grubbs' third generation catalyst (**G3'**, Scheme 1) possessing dramatic tolerance toward functional groups and providing polymers of narrow molecular weight distributions at very high monomer conversions, together with fast polymerization rates [43,61]. Furthermore, *endo*-substituted norbornenes are known to undergo ROMP significantly slower than their *exo* analogs, attributed either to steric reasons or to the chelating propensity of *endo*-substituted monomers [52,62-64]. It should be noted that our previous work showed that Grubbs' first (**G1**) and second generation (**G2**) catalysts were not sufficiently active to polymerize the ***endo*-NBAzl** diastereoisomer [52].

Monomer-to-initiator molar ratio ([**NBAzl**]/[**G3'**]) was varied from 50 to 500 (Table 1). After ROMP, full conversion of the monomer to polymer was observed within 24h for ([**NBAzl**]/[**G3'**] = 50 and 100 (runs 1 & 2, Table 1). Signals of the olefinic protons of **NBAzl** at δ = 5.86-6.25 ppm completely disappeared while broad cis/trans signals from the polymer backbone appeared at δ = 5.10–5.50 ppm. Increasing the monomer-to-initiator molar ratio to 500 led to a limited conversion even for a longer reaction time (Fig. S12 in SI). Nevertheless, initiator **G3'** induces a dramatically improved ROMP reactivity of *endo*-**NBAzl** compared to **G1** and **G2** and provides a quantitative monomer conversion for [**NBAzl**]/[**G3'**] = 100.

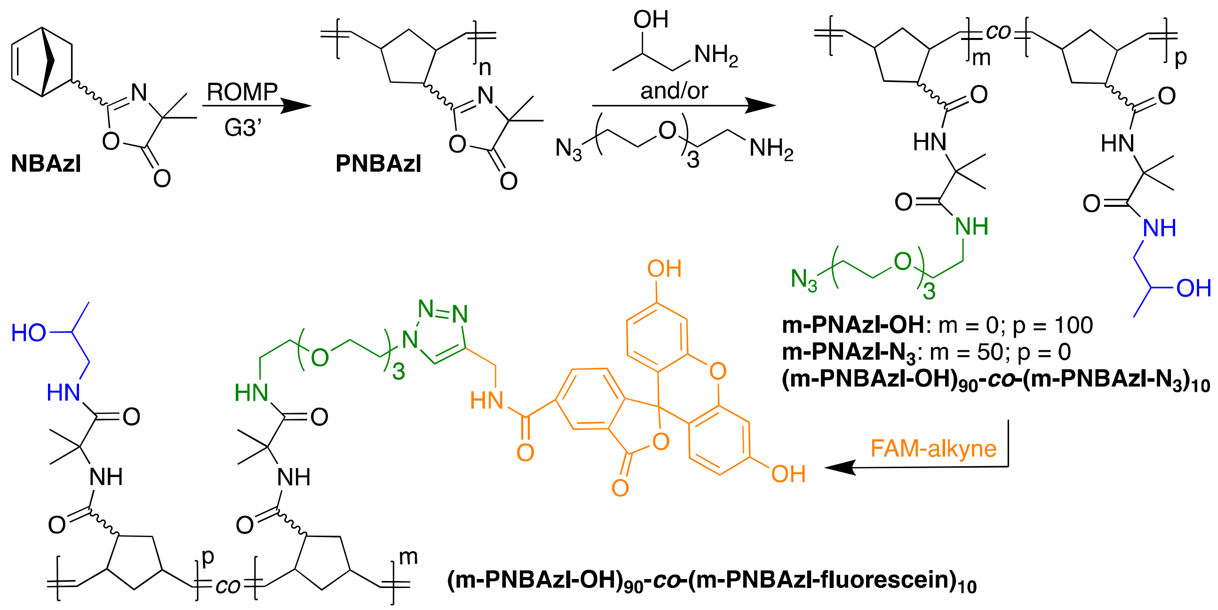

Scheme 1. Synthesis of clickable polynorbornene by postpolymerization modification of **PNBAzl** and fluorescein-carrying polynorbornene.

The calculated number-average degree of polymerization ($\overline{DP_{n,\ calc}}$) was determined by ^{1}H NMR, based on monomer conversion (Table 1). ^{1}H NMR end-group analysis has also been used to calculate the $\overline{DP_{n,\ NMR}}$ of the polynorbornenylazlactone (**PNBAzl**) from the ratio of the integrations of the olefinic protons signals of the polymer (labeled b and c, Fig. 1A) to the styrenic end-group protons signal at δ = 7.20–7.50 ppm (labeled z, Fig. 1A). These values are in close agreement with the expected $\overline{DP_{n,\ calc}}$ values (Table 1). Fourier Transform Infra-Red (FT-IR) spectroscopy shows absorption peaks at 1813 cm^{-1} (C=O stretching), 1668 cm^{-1} (C=N stretching), and 1203 cm^{-1} (C-O stretching), that are assigned to the azlactone ring in **PNBAzl** (Fig. 2A) [26].

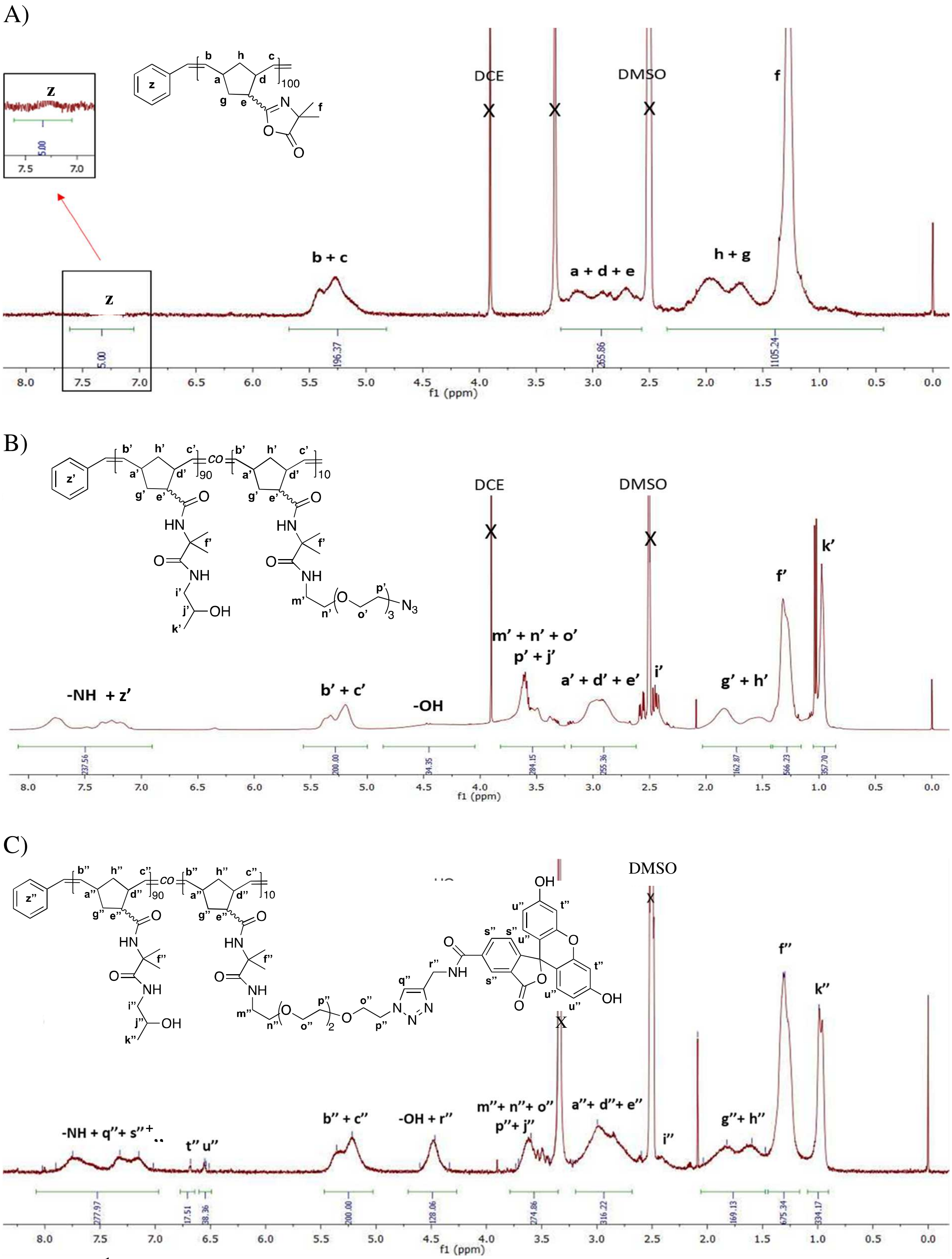

Fig. 1. [1]H NMR spectra of (A) **PNBAzl** (Table 1, run 2), (B) **(m-PNBAzl-OH)$_{90}$-*co*-(m-PNBAzl-N$_3$)$_{10}$** and (C) **(m-PNBAzl-OH)$_{90}$-*co*-(m-PNBAzl-fluorescein)$_{10}$**; solvent: DMSO-d$_6$.

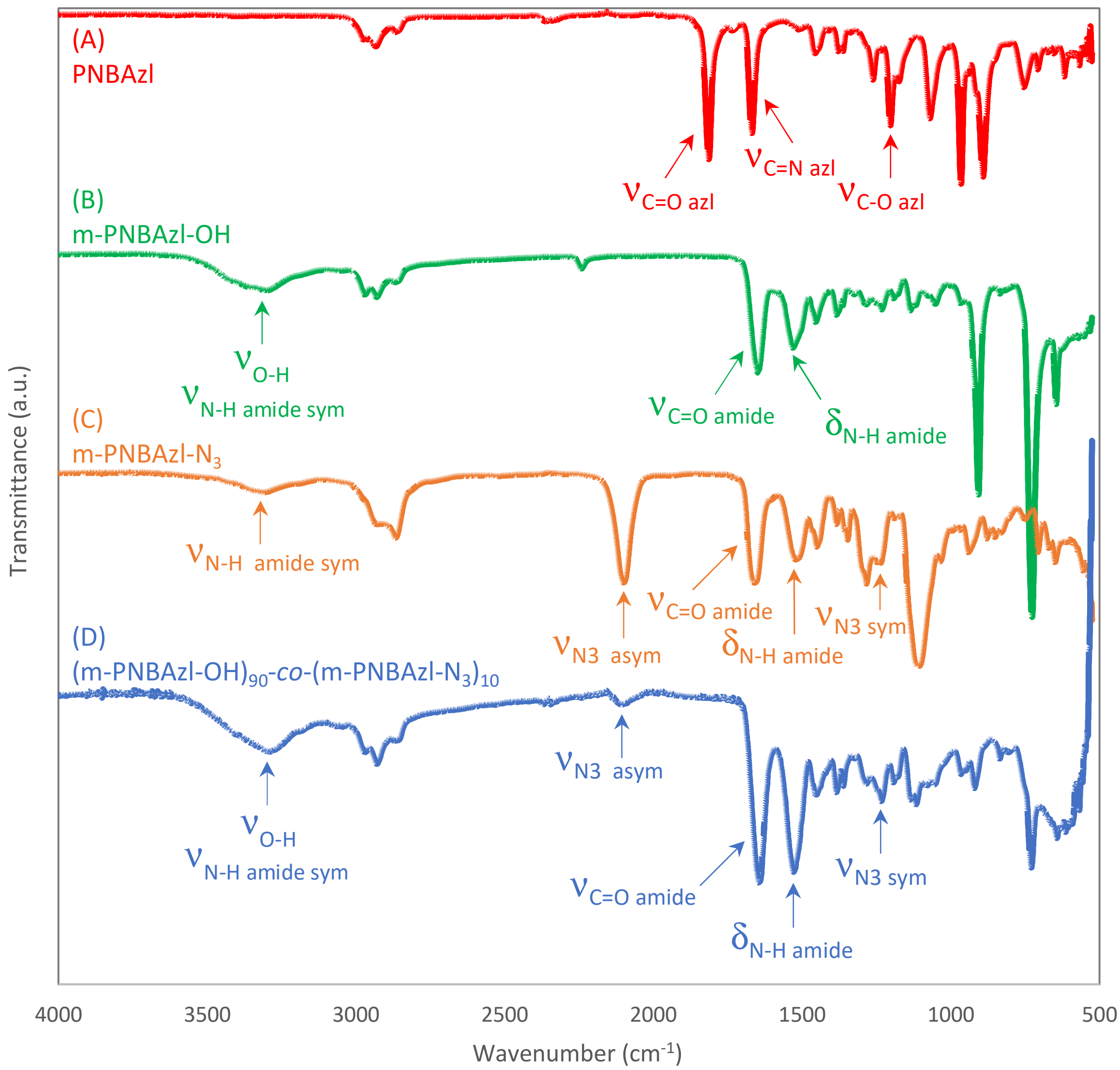

Fig. 2. ATR-FTIR spectra of (A) **PNBAzl**, (B) **m-PNBAzl-OH**, (C) **m-PNBAzl-N$_3$** and (D) **(m-PNBAzl-OH)$_{90}$-*co*-(m-PNBAzl-N$_3$)$_{10}$**.

Plot of number-average molar mass determined by size exclusion chromatography ($\overline{M_{n,SEC}}$) as a function of number-average degree of polymerization ($\overline{DP_{n,calc}}$ or $\overline{DP_{n,NMR}}$) values determined from NMR analysis gave linear trend lines (Fig. S13 in SI). The SEC traces of the **PNBAzl** displayed a monomodal symmetrical distribution with narrow dispersity values ranging from $Đ$ = 1.14 to 1.36 (Fig. S14 in SI). The precise control of both the molar mass and $Đ$ indicates that living ROMP of **NBAzl** was successfully achieved using **G3'** initiator.

Table 1. Characteristics of the polymers obtained by ROMP of **NBAzl** in DCE at 70 °C using **G3’** initiator for a reaction time of 24 h with varying monomer-to-initiator molar ratio.[a]

Run	[**NBAzl**]/[**G3’**]	Conv.[b] %	$\overline{DP_{n,calc}}$[c]	$\overline{M_{n,calc}}$[d] g.mol^{-1}	$\overline{DP_{n,NMR}}$[e]	$\overline{M_{n,NMR}}$[f] g.mol^{-1}	$\overline{M_{n,SEC}}$[g] g.mol^{-1}	Đ[g]
1	50	>99	50	10 370	53	11 000	9 900	1.17
2	100	>99	100	20 600	98	20 200	20 000	1.14
3	150	86	129	26 600	133	27 400	26 500	1.14
4	500	45	225	46 300	-[h]	-[h]	52 500	1.36

[a] Results are representative of at least duplicated experiments. [b] The monomer conversions were determined by comparing the integrations of alkene protons of the norbornene at δ = 5.86-6.25 ppm and the alkene protons of polymers at δ = 5.10-5.50 ppm from ^{1}H NMR spectra of the crude mixtures. [c] $\overline{DP_{n,calc}}$ = Conv. x ([**NBAzl**]$_0$/[**G3’**]$_0$). [d] $\overline{M_{n,calc}}$ = conv. x ([**NBAzl**]$_0$/[**G3’**]$_0$) x $M_{\mathbf{NBAzl}}$ + $M_{extr.}$ with $M_{\mathbf{NBAzl}}$ = 205 g.mol^{-1} and $M_{extr.}$ = 104 g.mol^{-1}. [e] Calculated from ^{1}H NMR spectra of the precipitated **PNBAzl** by comparing the peak areas of the olefinic protons signals of the polymer at δ = 5.10-5.50 ppm and the styrenic end-group protons signal at δ = 7.2–7.5 ppm. [f] $\overline{M_{n,NMR}}$ = ($\overline{DP_{n,NMR}}$ x $M_{\mathbf{NBAzl}}$) + $M_{extr.}$ with $M_{\mathbf{NBAzl}}$ = 205 g.mol^{-1} and $M_{extr.}$ = 104 g.mol^{-1}. [g] Determined by SEC in tetrahydrofuran (THF) using a RI detector, calibrated with linear polystyrene (PS) standards. [h] not observed.

First-order kinetics were observed for monomer conversion in the ROMP of **NBAzl** at 70°C in DCE using **G3’** for [**NBAzl**]/[**G3’**] = 100 (Fig. 3A). The first- and the second-order self-propagation rate constant, (k_p^{app} and k_p, respectively) were calculated according to equation (1) [65]:

$$-\frac{d[M]_t}{dt} = k_p^{app}[M]_t = k_p[G3']_0[M]_t \quad (1)$$

These values are listed in Table 2 together with values taken from the literature for ROMP of *endo*-substituted norbornene with **G3’** as initiator [66,67]. **NBAzl** has a much lower reactivity in ROMP even at high temperature than *endo*-substituted norbornenes, already reported as poor reactive monomers because of their bulky steric profile (run 1 *vs.* runs 2-4, Table 2) [62]. Even if the mainly present *endo*-**NBAzl** polymerizes more slowly than its *exo*-counterpart, the electronic effect of the azlactone group plays a crucial role in inhibiting the ROMP of **NBAzl** with a k_p of the same order of magnitude than for the *N*-(2,2,6,6-tetramethylpiperidine-1-oxyl)-*exo*-norbornene-5,6-dicarboximide (runs 1 & 5, Table 2).

Table 2. Kinetic data for ROMP of **NBAzl** and *endo*-substituted norbornenes using **G3’** as the initiator with monomer-to-initiator molar ratio = 100.

Entry	Monomer	Solvent	Temperature °C	k_p $s^{-1}.L.mol^{-1}$	Ref.
1	**NBAzl**	DCE	70	0.005	This work
2	*endo*,*endo*-norbornenyl-2,3-dimethyl ester	DCM	25	2.24	[66]
3	*endo*,*endo*-norbornenyl-2,3-di-n-butyl ester	DCM	25	0.362	[66]
4	*N*-*tert*-butyl-*endo*-norbornene-5,6-dicarboximide	DCM	25	0.782	[66]
5	*N*-TEMPO-*exo*-norbornene-5,6-dicarboximide[a]	DCM	25	0.006	[67]

[a)] TEMPO: 2,2,6,6-tetramethylpiperidine-1-oxyl.

3.2. Postpolymerization modification of PNBAzl

The “click-like” nature of the amine-reactive azlactone functionality [12,13,68] was then exploited to functionalize **PNBAzl** by treatment with primary amine-based nucleophiles. This “grafting to” strategy applied to the **PNBAzl** platform leads to new side chain-functionalized materials. **PNBAzl** was click grafted with 1-aminopropan-2-ol and 11-azido-3,6,9-trioxaundecan-1-amine at a feed molar ratio of 90:10. This material has been designed with (1) hydroxyl side groups and amide linkages to promote hydrogen bonding with water molecules to facilitate polymer hydration [69,70] and (2) azide side groups for a further functionalization through copper-catalyzed alkyne–azide cycloaddition (CuAAC) click reaction [71].

The postpolymerization modification (PPM) of **PNBAzl** was first investigated with 1-aminopropan-2-ol. The reaction was conducted in deuterated chloroform ($CDCl_3$) by using a 1.2:1 molar ratio of 1-aminopropan-2-ol to the azlactone ring at 25 °C for 16 h with a polymer concentration of 100 g/L. The ^1H NMR spectrum of the **PNBAzl** modified with 1-aminopropan-2-ol (**m-PNBAzl-OH**) showed two individual signal peaks of NH protons in the amides at 7.80 and 7.18 ppm (labeled i and i’, Fig. S3 in SI) together with a multiplet signal of the methyl protons of the 1-aminopropan-2-ol moiety at 1.00 ppm (labeled l, Fig. S3 in SI). The PPM proceeded in a quasi-quantitative way as ascertained by comparing the ratio of the integration areas of the olefin protons signals of the polymer backbone at 5.21 and 5.35 ppm (labeled b and c, Fig. S3 in SI) and of the methyl group signal of the isopropanol side end-group at 1.00 ppm (labeled l, Fig. S3 in SI). Complete conversion of the azlactone ring was also confirmed by FT-IR spectroscopy, which indicated complete disappearance of the azlactone C=O (at 1813 cm^{-1}) and C=N (at 1668 cm^{-1}) stretching bands and the appearance of bands attributed to amide N–H symmetric stretching (3304 cm^{-1}) and N–H bending (1531 cm^{-1}) (Fig. 2B) [24].

The PPM of **PNBAzl** with 11-azido-3,6,9-trioxaundecan-1-amine required more drastic conditions to drive the reaction toward high conversion and was performed in DCE by using a 1.1:1 molar ratio of 11-azido-3,6,9-trioxaundecan-1-amine to the azlactone ring at 50°C for 3 h with a polymer concentration of 100 g/L. The ^{1}H NMR spectrum of the **PNBAzl** modified with 11-azido-3,6,9-trioxaundecan-1-amine (**m-PNBAzl-N$_3$**) shows signals at 6.92 ppm (N-H protons; Fig. S6 in SI) and between 3.25 and 3.87 ppm (CH_2-CH_2-O protons), indicating that the click grafting actually occurs. The integration of the signals of the olefinic protons at 5.21 and 5.31 ppm (labeled b and c, Fig. S6 in SI) and of ethylene oxide protons between 3.25 and 3.87 ppm (labeled n, m, o and p, Fig. S6 in SI) gave a ratio of 1/8.5, which indicates a quasi-quantitative modification. In the FT-IR spectrum of **m-PNBAzl-N$_3$** (Fig. 2C), the absorption peaks at 1813 cm^{-1} and at 1668 cm^{-1}, ascribed to stretch vibration mode of C=O and C=N of the azlactone, respectively, disappeared after PPM, while the stretching vibration peak of N-H emerged at 3310 cm^{-1}, together with asymmetric and symmetric stretching vibration peaks of azides at 2100 cm^{-1} and 1235 cm^{-1}, respectively [72].

PNBAzl was then sequentially transformed into the corresponding **(m-PNBAzl-OH)$_{90}$-*co*-(m-PNBAzl-N$_3$)$_{10}$** copolymer (Scheme 1) according to a two steps one-pot procedure.

PNBAzl was first reacted with 11-azido-3,6,9-trioxaundecan-1-amine in DCE at 50°C for 3h using a molar ratio [amine]/[azlactone] = 10 % and a polymer concentration of 100 g/L. Subsequently, 1-aminopropan-2-ol was added to the reaction mixture to react with the remaining unreacted azlactone groups at 50°C for 4h. The copolymer was then purified by dialysis and analyzed by SEC in *N*,*N*-dimethylformamide (DMF). The SEC trace displayed a very broad distribution, resulting in a dispersity value higher than 2 (Fig. S15A in SI). The broadness of the peak may be attributed to undesired coupling reactions between the hydroxyl functionality of 1-aminopropan-2-ol and the azlactone ring, leading to partial crosslinking. Since thermally activated alcohol-azlactone reactions have already been reported [73], the temperature of the reaction was lowered from 50°C to 25°C before the addition of 1-aminopropan-2-ol, reducing undesired coupling reactions (Fig. S15B in SI). Ring-opening reactions of azlactone involving alcohols usually require the addition of an acid or base [11]. It can be inferred that 1-aminopropan-2-ol is basic enough to act as a catalyst for the nucleophilic addition of alcohol on the azlactone moiety. It has thus been shown that amino alcohols are more reactive than primary amines during the aminolysis of esters [74-77]. Fortunately, the undesired coupling reactions were suppressed by decreasing both the temperature and the polymer concentration from 100 g/L to 5 g/L, as ascertained by the monomodal distribution of the SEC chromatogram with a narrow dispersity of 1.19 (Fig. S15C in SI). A shift to lower elution time in SEC occurs after sequential modification of **PNBAzl**, which is consistent with the increase in molar mass and hydrodynamic volume resulting from the grafting reaction (Fig. S16A *vs.* S16B in SI). In the FT-IR spectrum (Fig. 2D), the strong carbonyl band of the azlactone ring at 1813 cm^{-1} fully disappears, indicating complete modification of the azlactone. The strong bands at 3288 cm^{-1}, 1646 cm^{-1}, and 1528 cm^{-1} are attributed to N-H symmetric stretching, C=O asymmetric stretching, and N-H bending of secondary amides resulting from the effective PPM of **PNBAzl** with primary amines, respectively. The presence of the azido functionality is ascertained by the N_3 asymmetric stretching band at 2104 cm^{-1}. In addition, characteristic bands of carboxylate functionality (expected around 1560 cm^{-1}) were not detected, indicating a quantitative PPM and that hydrolysis of azlactone groups did not occur [21]. The ^{1}H NMR spectrum of **(m-PNBAzl-OH)$_{90}$-*co*-(m-PNBAzl-N$_3$)$_{10}$** is shown in Fig. 1B. The appearance of the methyl group signal of 1-aminopropan-2-ol at 1.00 ppm (labeled k', Fig. 1B) indicates that the modification with 1-aminopropan-2-ol proceeded to high conversion. Furthermore, the peaks attributed to the 11-azido-3,6,9-trioxaundecan-1-amine functionalized units appear at 3.25-3.86 ppm (labeled m', n', o' and p', Fig. 1B). Integration of these signals leads to a 88:12 molar ratio of the pendent 1-aminopropan-2-ol and 11-azido-3,6,9-trioxaundecan-1-amine groups, respectively, in good agreement with the molar ratio of reagents used during the PPM. It should be emphasized that this click methodology provides the key advantage of circumventing the known incompatibility of the alkyl azide side group in the monomer repeat unit with ruthenium-based catalysts [58,59]. Indeed, ROMP polymers with azide groups in the side chain cannot be prepared by direct ROMP of the corresponding azide monomers, thus requiring an additional PPM by nucleophilic substitution of an halogen atom using sodium azide, which is not an atom-economic reaction [48,57].

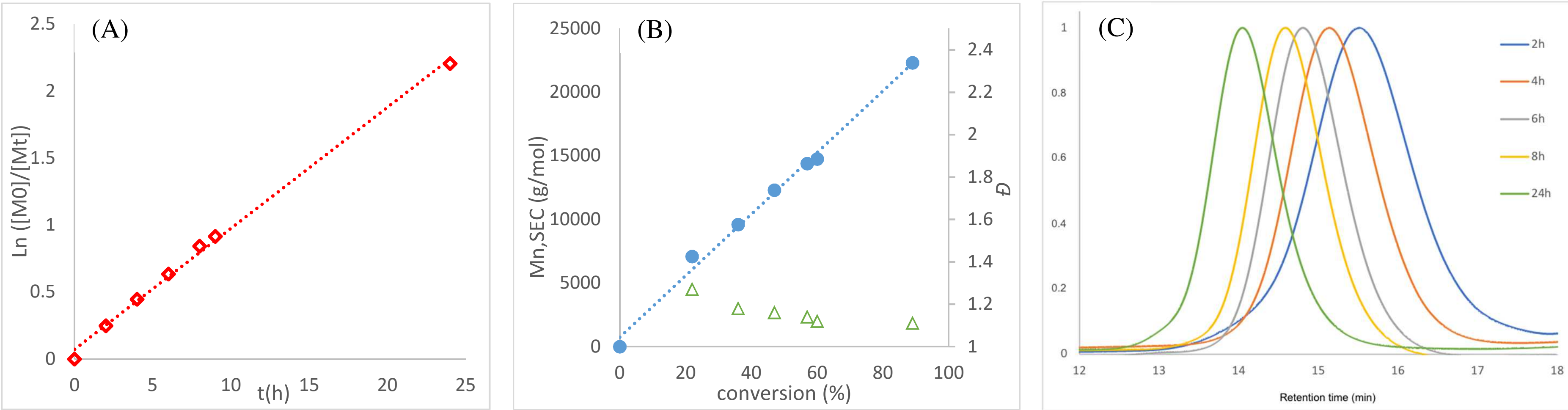

Fig. 3. (A) Kinetic plot - ln($[M]_t/[M]_0$) as a function of reaction time (B) $\overline{M_{n,SEC}}$ and *Đ* versus conversion of **NBAzl**, and (C) SEC traces of crude polymers at different conversions of monomer for the ROMP of **NBAzl** using **G3'** as the initiator with an initial monomer concentration of 0.05 mol.L^{-1} and a $[M]_0/[I]_0$ ratio of 100 at 70 °C in DCE (THF eluent; RI detector).

3.3. Fluorescein-carrying modified PNBAzl

Applying click chemistry reactions to build bio-hybrid copolymers is a well-established route toward highly functionalized bioconjugates [4]. The feasibility and efficiency of the click CuAAC applied to **(m-PNBAzl-OH)$_{90}$-*co*-(m-PNBAzl-N$_3$)$_{10}$** was herein evaluated using a labeled alkynyl-modified fluorescein (FAM-alkyne). Briefly, **(m-PNBAzl-OH)$_{90}$-*co*-(m-PNBAzl-N$_3$)$_{10}$** was reacted with FAM-alkyne in DMF at room temperature in the presence of a catalytic amount of Cu(I)Br with *N,N,N',N',N''*-pentamethyldiethylenetriamine (PMDETA) as the ligand for 24 h (Scheme 1). Purification was conveniently achieved by flash column chromatography on neutral alumina. After dialysis against water and lyophilization, **(m-PNBAzl-OH)$_{90}$-*co*-(m-PNBAzl-fluorescein)$_{10}$** was obtained as a yellow solid. The ^{1}H NMR spectrum in Fig. 1C clearly shows that new peaks $H_{r''}$, $H_{t''}$ and $H_{u''}$ appeared after coupling reaction at δ = 4.33-4.61, 6.54 and 6.68 ppm, respectively, in addition to the typical proton signals of the modified **PNBAzl** backbone. The peak $H_{r''}$ was assigned to the methylene group next to the nitrogen of the triazole groups and the peaks $H_{t''}$ and $H_{u''}$ were assigned to the aromatic protons of FAM-alkyne. The average grafting efficiency of FAM-alkyne to the backbone of modified **PNBAzl** was calculated using ^{1}H NMR spectrum from the integration areas of the olefin protons signals of the polymer backbone between 5.04 and 5.47 ppm (labeled b" and c", Fig. 1C) and the aromatic proton of FAM-alkyne (labeled t" and u'', Fig. 1C at 6.54 and 6.68 ppm). The grafting efficiency was about 93%. Moreover, the SEC overlay (Fig. 4) revealed a peak at 517 nm of the UV detector of the SEC, corresponding to the fluorescein absorbance and demonstrating that the N_3 functionality has reacted. This facile, but versatile methodology will be applicable for the synthesis of a wide range of (bio)-functionalized polymers and polymer libraries based on the **PNBAzl** platform through highly efficient click-type reactions.

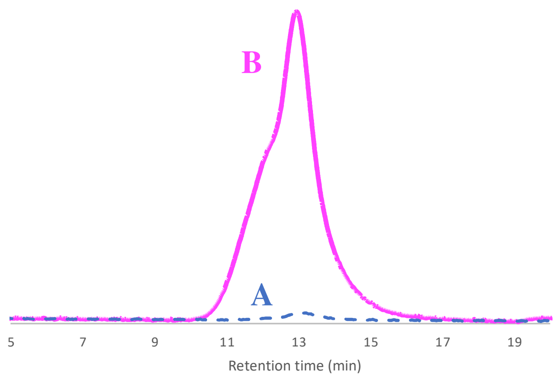

Fig. 4. Overlaid SEC chromatograms (DMF eluent) from the UV detector at 517 nm for (A) **(m-PNBAzl-OH)$_{90}$-*co*-(m-PNBAzl-N$_3$)$_{10}$** (dashed line) and (B) **(m-PNBAzl-OH)$_{90}$-*co*-(m-PNBAzl-fluorescein)$_{10}$** (full line).

4. Conclusions

In summary, this paper reports the first synthesis of well-defined poly(norbornenyl azlactone) (**PNBAzl**) using the Ru-based **G3'** catalyst without requiring the tedious separation of the mixture of stereoisomers from the corresponding norbornenyl azlactone (**NBAzl**) monomer. The facile PPM of the so-obtained **PNBAzl** by azlactone ring-opening was demonstrated using amine nucleophiles, including azido-functionalized oligoethylene glycol-amine, leading to functional ROMP polymers that cannot be accessed by ROMP of azido-functionalized norbornenes. In addition, the easy access, on a multigram scale, to the corresponding **NBAzl** monomer from inexpensive and commercially available reagents makes this method particularly attractive. The ability of the resulting azido-functionalized polymers to enter further alkyne-azide click modification was demonstrated using an alkynyl-fluorescein as a model. The **PNBAzl** reported in this work thus provides a unique platform to prepare new ROMP-based polymers through sequential PPM with complete atom economy using a wide range of nucleophiles with multiple applications, including new functional materials and bioconjugates for biology and medicine.

Data availability

The raw data required to reproduce these findings are available from the corresponding authors upon request.

Acknowledgments

We thank Mireille Barthe and Alexandre Bénard for SEC analyses, Fabien Boeda and Emilie Choppé for catalyst synthesis and technical assistance, and Sullivan Bricaud for NMR analyses. We acknowledge financial support from Le Mans University and CNRS. This manuscript is a tribute to the 50 years anniversary of the French Polymer Group (Groupe Français des Polymères, GFP).

References

[1] E. Blasco, M.B. Sims, A.S. Goldmann, B.S. Sumerlin, C. Barner-Kowollik, 50th Anniversary Perspective: Polymer Functionalization, Macromolecules 50 (2017) 5215–5252. https://doi.org/10.1021/acs.macromol.7b00465.

[2] T. Kubo, C.P. Easterling, R.A. Olson, B.S. Sumerlin, Synthesis of multifunctional homopolymers via sequential post-polymerization reactions, Polym. Chem. 9 (2018) 4605–4610. https://doi.org/10.1039/c8py01055b.

[3] J. Romulus, J.T. Henssler, M. Weck, Post-polymerization modification of block copolymers, Macromolecules 47 (2014) 5437–5449. https://doi.org/10.1021/ma5009918.

[4] P. Theato, H.A. Klok, Functional Polymers by Post-Polymerization Modification, VCH, Weinheim, 2013. https://doi.org/10.1002/9783527655427.

[5] K.A. Günay, P. Theato, H.A. Klok, Standing on the shoulders of Hermann Staudinger: Post-polymerization Modification from Past to Present, J. Polym. Sci., Part A: Polym. Chem. 51 (2013) 1–28. https://doi.org/10.1002/pola.26333.

[6] M. Gauthier, M. Gibson, H.A. Klok, Synthesis of functional polymers by post-polymerization modification, Angew. Chem., Int. Ed. 48 (2009) 48–58. https://doi.org/10.1002/anie.200801951.

[7] L.A. Bultema, X. Huang, D.D. Brauer, P. Theato, Polymer Functionalization in: M. Jafar Mazumder, H. Sheardown, A. Al-Ahmed (Eds.), Functional Polymers. Polymers and Polymeric Composites: A Reference Series, Springer, Cham, 2019, pp. 1–51. https://doi.org/10.1007/978-3-319-92067-2_2-1.

[8] A. Das, P. Theato, Activated Ester Containing Polymers: Opportunities and Challenges for the Design of Functional Macromolecules, Chem. Rev. 116 (2016) 1434–1495. https://doi.org/10.1021/acs.chemrev.5b00291.

[9] P. Theato, Synthesis of well-defined polymeric activated esters. J. Polym. Sci., Part A: Polym. Chem. 46 (2008) 6677–6687. https://doi.org/10.1002/pola.22994.

[10] L. He, K. Szameit, H. Zhao, U. Hahn, P. Theato, Postpolymerization Modification Using Less Cytotoxic Activated Ester Polymers for the Synthesis of Biological Active Polymers, Biomacromolecules 15 (2014) 3197–3205. https://doi.org/10.1021/bm500902t.

[11] S.M. Heilmann, J.K. Rasmussen, L.R. Krepski, Chemistry and Technology of 2-Alkenyl Azlactones, J. Polym. Sci., Part A: Polym. Chem. 39 (2001) 3655–3677. https://doi.org/10.1002/pola.10007.

[12] M.E. Buck, D.M. Lynn, Azlactone-functionalized polymers as reactive platforms for the design of advanced materials: Progress in the last ten years, Polym. Chem. 3 (2012) 66–80. https://doi.org/10.1039/c1py00314c.

[13] H.T. Ho, M.E. Levere, D. Fournier, V. Montembault, S. Pascual and L. Fontaine, Introducing the Azlactone Functionality into Polymers through Controlled Radical Polymerization: Strategies and Recent Developments, Aust. J. Chem. 65 (2012) 970–977. https://doi.org/10.1071/CH12192.

[14] H.T. Ho, A. Bénard, G. Forcher, M. Le Bohec, V. Montembault, S. Pascual, L. Fontaine, Azlactone-based heterobifunctional linkers with orthogonal clickable groups: Efficient tools for bioconjugation with complete atom economy, Org. Biomol. Chem. 16 (2018) 7124–7128. https://doi.org/10.1039/c8ob01807c.

[15] M. Pantin, J. Caillé, F. Boeda, L. Fontaine, M. Pearson-Long, P. Bertus, Heteromultifunctional oxazolones as versatile linkers for click chemistry reactions Eur. J. Org. Chem. (2019) 7359–7366. https://doi.org/10.1002/ejoc.201901350.

[16] R. Kakuchi, K. Wongsanoh, V.P. Hoven, P. Theato, Activation of stable polymeric esters by using organo-activated acyl transfer reactions, J. Polym. Sci. A Polym. Chem. 52 (2014) 1353–1358. https://doi.org/10.1002/pola.27124.

[17] C.P. Easterling, T. Kubo, Z.M. Orr, G.E. Fanucci, B.S. Sumerlin, Synthetic upcycling of polyacrylates through organocatalyzed post-polymerization modification, Chem. Sci. 8 (2017) 7705–7709. https://doi.org/10.1039/C7SC02574B.

[18] J.F.R. Van Guyse, J. Verjans, S. Vandewalle, K. De Bruycker, F.E. Du Prez, R. Hoogenboom, Full and Partial Amidation of Poly(methyl acrylate) as Basis for Functional Polyacrylamide (Co)Polymers, Macromolecules 52 (2019) 5102–5109. https://doi.org/10.1021/acs.macromol.9b00399.

[19] C. Hils, E. Fuchs, F. Eger, J. Schöbel, H. Schmalz, Converting Poly(Methyl Methacrylate) into a Triple-Responsive Polymer, Chem. Eur. J. 26 (2020) 5611–5614. https://doi.org/10.1002/chem.202000485.

[20] M.W. Jones, S.J. Richards, D.M. Haddleton, M.I. Gibson, Poly(azlactone)s: versatile scaffolds for tandem post-polymerisation modification and glycopolymer synthesis, Polym. Chem. 4 (2013) 717–723. https://doi.org/10.1039/c2py20757e.

[21] Y Zhu, J.Y. Quek, A.B. Lowe, P.J. Roth, Thermoresponsive (Co)polymers through Postpolymerization Modification of Poly(2-vinyl-4,4-dimethylazlactone), Macromolecules 46 (2013) 6475–6484. https://doi.org/10.1021/ma401096r.

[22] J.Y. Quek, X. Liu, T.P. Davis, P.J. Roth, A.B. Lowe, RAFT-prepared α-difunctional poly(2-vinyl-4,4-dimethylazlactone)s and their derivatives: synthesis and effect of end-groups on aqueous inverse temperature solubility, Polym. Chem. 6 (2015) 118–127. https://doi.org/10.1039/C4PY01108B.

[23] Y. Pei, O.R. Sugita, J.Y. Quek, P.J. Roth, A.B. Lowe, pH-, thermo- and electrolyte-responsive polymer gels derived from a well-defined, RAFT-synthesized, poly(2-vinyl-4,4-dimethylazlactone) homopolymer via one-pot post-polymerization modification, Eur. Polym. J. 62 (2015) 204–213. https://doi.org/10.1016/j.eurpolymj.2014.11.025.

[24] Y. Zhu, R. Batchelor, A.B. Lowe, P.J. Roth, Design of Thermoresponsive Polymers with Aqueous LCST, UCST, or Both: Modification of a Reactive Poly(2-vinyl-4,4-dimethylazlactone) Scaffold, Macromolecules 49 (2016) 672–680. https://doi.org/10.1021/acs.macromol.5b02056.

[25] A. Guyomard, D. Fournier, S. Pascual, L. Fontaine, J.F. Bardeau, Preparation and characterization of azlactone functionalized polymer supports and their application as scavengers, Eur. Polym. J. 40 (2004) 2343–2348. https://doi.org/10.1016/j.eurpolymj.2004.05.005.

[26] H.T. Ho, F. Leroux, S. Pascual, V. Montembault, L. Fontaine, Amine-Reactive Polymers Synthesized by RAFT Polymerization Using An Azlactone Functional

Trithiocarbonate RAFT Agent, Macromol. Rapid Commun. 33 (2012) 1753–1758. https://doi.org/10.1002/marc.201200367.

[27] B.S. Lokitz, J. Wei, J.P. Hinestrosa, I. Ivanov, J.F. Browning, J.F. Ankner, S.M. Kilbey II, J.M. Messman, Manipulating Interfaces through Surface Confinement of Poly(glycidyl methacrylate)-block-poly(vinyldimethylazlactone), a Dually Reactive Block Copolymer, Macromolecules 45 (2012) 6438–6449. https://doi.org/10.1021/ma300991p.

[28] Y. Li, H.T.T. Duong, M. Jones, J.S. Basuki, J. Hu, C. Boyer, T.P. Davis, Selective Postmodification of Copolymer Backbones Bearing Different Activated Esters with Disparate Reactivities, ACS Macro Lett. 2 (2013) 912–917. https://doi.org/10.1021/mz4004375.

[29] M.C.D. Carter, J. Jennings, V. Appadoo, D.M. Lynn, Synthesis and Characterization of Backbone Degradable Azlactone-Functionalized Polymers, Macromolecules 49 (2016) 5514–5526. https://doi.org/10.1021/acs.macromol.6b01212.

[30] C. Chauveau, E. Vanbiervliet, S. Fouquay, G. Michaud, F. Simon, J.F. Carpentier, S.M. Guillaume, Azlactone Telechelic Polyolefins as Precursors to Polyamides: A Combination of Metathesis Polymerization and Polyaddition Reactions Macromolecules 51 (2018) 8084–8099. https://doi.org/10.1021/acs.macromol.8b01628.

[31] J.J. Glass, Y. Li, R. De Rose, A.P.R. Johnston, E.I. Czuba, S.Y. Khor, J.F. Quinn, M.R. Whittaker, T.P. Davis, S.J. Kent, Thiol-Reactive Star Polymers Display Enhanced Association with Distinct Human Blood Components, ACS Appl. Mater. Interfaces 9 (2017) 12182−12194. https://doi.org/10.1021/acsami.6b15942.

[32] M.M. Wancura, Q. Anex-Ries, A.L. Carroll, A.P. Garcia, P. Hindocha, M.E. Buck, Fabrication, Chemical Modification, and Topographical Patterning of Reactive Gels

Assembled from Azlactone-Functionalized Polymers and a Diamine, J. Polym. Sci. Part A: Polym. Chem. 55 (2017) 3185–3194. https://doi.org/10.1002/pola.28664.

[33] J.L. Grace, M. Amado, J.C. Reid, A.G. Elliott, C.B. Landersdorfer, N.P. Truong, K. Kempe, M.A. Cooper, T.P. Davis, V. Montembault, S. Pascual, L. Fontaine, T. Velkov, J.F. Quinn, M.R. Whittaker, An optimised Cu(0)-RDRP approach for the synthesis of lipidated oligomeric vinyl azlactone: Toward a versatile antimicrobial materials screening platform, J. Mater. Chem. B 7 (2019) 6796–6809. https://doi.org/10.1039/C9TB01624D.

[34] C. Kanimozhi, M.J. Shea, J. Ko, W. Wei, P. Huang, M.S. Arnold, P. Gopalan, Removable Nonconjugated Polymers To Debundle and Disperse Carbon Nanotubes, Macromolecules 52 (2019) 4278–4286. https://doi.org/10.1021/acs.macromol.9b00352.

[35] X. Yu, A. Herberg, D. Kuckling, Azlactone-functionalized smart block copolymers for organocatalyst immobilization, Eur. Polym. J. 120 (2019) 109207. https://doi.org/10.1016/j.eurpolymj.2019.08.034.

[36] M. Le Bohec, M. Banère, S. Piogé, S. Pascual, L. Benyahia, L. Fontaine, Sol-gel reversible metallo-supramolecular hydrogels based on a thermoresponsive double hydrophilic block copolymer. Polym. Chem. 7 (2016) 6834–6842. https://doi.org/10.1039/C6PY01639A.

[37] Y. Prai-In, K. Tankanya, B. Rutnakornpituk, U. Wichai, V. Montembault, S. Pascual, L. Fontaine, M. Rutnakornpituk, Azlactone functionalization of magnetic nanoparticles using ATRP and their bioconjugation, Polymer 53 (2012) 113–120. https://doi.org/10.1016/j.polymer.2011.11.021.

[38] H.T. Ho, M.E. Levere, S. Pascual, V. Montembault, A. Caruso, N. Casse, L. Fontaine, Thermoresponsive Block Copolymers Containing Reactive Azlactone Groups and

their Bioconjugation with Lysozyme, Polym. Chem. 4 (2013) 675–685. https://doi.org/10.1039/C2PY20714A.

[39] V. Delplace, S. Harrison, H.T. Ho, A. Tardy, Y. Guillaneuf, S. Pascual, L. Fontaine, J. Nicolas, One-Step Synthesis of Azlactone-Functionalized SG1-Based Alkoxyamine for Nitroxide-Mediated Polymerization and Bioconjugation, Macromolecules 48 (2015) 2087–2097. https://doi.org/10.1021/acs.macromol.5b00178.

[40] S.K. Schmitt, D.J. Trebatoski, J.D. Krutty, A.W. Xie, B. Rollins, W.L. Murphy, P. Gopalan, Peptide Conjugation to a Polymer Coating via Native Chemical Ligation of Azlactones for Cell Culture, Biomacromolecules 17 (2016) 1040−1047. https://doi.org/10.1021/acs.biomac.5b01682.

[41] J.S. Kim, A.R. Sirois, A.J. Vazquez Cegla, E. Jumai'an, N. Murata, M.E. Buck, S.J. Moore, Protein–Polymer Conjugates Synthesized Using Water-Soluble Azlactone-Functionalized Polymers Enable Receptor-Specific Cellular Uptake toward Targeted Drug Delivery, Bioconjugate Chem. 30 (2019) 1220–1231. https://doi.org/10.1021/acs.bioconjchem.9b00155.

[42] J. Liebscher, J. Teßmar, J. Groll, In Situ Polymer Analogue Generation of Azlactone Functions at Poly(oxazoline)s for Peptide Conjugation, Macromol. Chem. Phys. 221 (2020) 1900500. https://doi.org/10.1002/macp.201900500.

[43] C. W. Bielawski, R. H. Grubbs, Living ring-opening metathesis polymerization, Prog. Polym. Sci. 32 (2007) 1–29. https://doi.org/10.1016/j.progpolymsci.2006.08.006.

[44] R. R. Schrock, Synthesis of Stereoregular Polymers through Ring-Opening Metathesis Polymerization, Acc. Chem. Res. 47 (2014) 2457–2466. https://doi.org/10.1021/ar500139s.

[45] G. Morandi, G. Mantovani, V. Montembault, D.M. Haddleton, L. Fontaine, Synthesis of graft copolymers from alpha-oxanorbornenyl macromonomers, New J. Chem. 31 (2007) 1826–1829. https://doi.org/10.1039/B705245F.

[46] D. Le, G. Morandi, S. Legoupy, S. Pascual, V. Montembault, L. Fontaine, Cyclobutenyl macromonomers: Synthetic strategies and ring-opening metathesis polymerization, Eur. Polym. J. 49 (2013) 972–983. https://dx.doi.org/10.1016/j.eurpolymj.2013.01.008.

[47] M.S. Messina, K.M.M. Messina, A. Bhattacharya, H.R. Montgomery, H.D. Maynard, Preparation of biomolecule-polymer conjugates by grafting-from using ATRP, RAFT, or ROMP, Progr. Polym. Sci. 100 (2020) 101186. https://doi.org/10.1016/j.progpolymsci.2019.101186.

[48] J.A. Johnson, Y.Y. Lu, A.O. Burts, Y.H. Lim, M.G. Finn, J.T. Kobertstein, N.J. Turro, D.A. Tirell, R.H. Grubbs, Core-clickable PEG-*branch*-azide bivalent-bottle-brush polymers by ROMP: grafting-through and clicking-to, J. Am. Chem. Soc. 133 (2011) 559–566. https://doi.org/10.1021/ja108441d.

[49] L.E. Strong, L.L. Kiessling, A General Synthetic Route to Defined, Biologically Active Multivalent Arrays, J. Am. Chem. Soc. 121 (1999) 6193–6196. https://doi.org/10.1021/ja990223t.

[50] S.L. Mangold, R.T. Carpenter, L.L. Kiessling, Synthesis of Fluorogenic Polymers for Visualizing Cellular Internalization, Org. Lett. 10 (2008) 2997–3000. https://doi.org/10.1021/ol800932w.

[51] N. Vogel, P. Theato, Controlled Synthesis of Reactive Polymeric Architectures Using 5□Norbornene□2□carboxylic Acid Pentafluorophenyl Ester, Macromol. Symp. 249-250 (2007) 383–391. https://doi.org/10.1002/masy.200750408.

[52] V. Lapinte, J.C. Brosse, L. Fontaine, Synthesis and Ring-Opening Metathesis Polymerization (ROMP) of (±)-*endo*- and (±)-*exo*-Norbornenylazlactone using Ruthenium Catalysts, Macromol. Chem. Phys. 205 (2004) 824–833. https://doi.org/10.1002/macp.200300120.

[53] V. Lapinte, L. Fontaine, V. Montembault, I. Campistron, D. Reyx, Ring-Opening Metathesis Polymerization (ROMP) of isomerically pure functional monomers and Acyclic Diene Metathesis depolymerization (retro-ADMET) of functionalized polyalkenamers, J. Mol. Catal. A: Chem. 190 (2002) 117–129. https://doi.org/10.1016/S1381-1169(02)00229-7.

[54] A.F. Jacobine, D.M. Glaser, J.P. Grabek, D. Mancini, M. Masterson, S.T. Nakos, M.A. Rakas, J.G. Woods, Photocrosslinked norbornene-thiol copolymers: Synthesis, mechanical properties, and cure studies, J. Appl. Polym. Sci. 45 (1992) 471–485. https://doi.org/10.1002/app.1992.070450312.

[55] C.W. Bielawski, R.H. Grubbs, Highly efficient ring-opening metathesis polymerization (ROMP) using new ruthenium catalysts containing *N*-heterocyclic carbene ligands, Angew. Chem. Int. Ed. 39 (2000) 2903–2906. https://doi.org/10.1002/1521-3773(20000818)39:16<2903::AID-ANIE2903>3.0.CO;2-Q.

[56] M. Schaefer, N. Hanik, A.F.M. Kilbinger, ROMP Copolymers for Orthogonal Click Functionalizations, Macromolecules 45 (2012) 6807–6818. https://doi.org/10.1021/ma301061z.

[57] S.K. Yang, M. Weck, Modular Covalent Multifunctionalization of Copolymers, Macromolecules 41 (2008) 346–351. https://doi.org/10.1021/ma702052k.

[58] Y. Xia, R. Verduzco, R.H. Grubbs, J.A. Kornfield, Well-Defined Liquid Crystal Gels from Telechelic Polymers, J. Am. Chem. Soc. 130 (2008) 1735−1740. https://doi.org/10.1021/ja077192j.

[59] A. Leitgeb, J. Wappel, C. Slugovc, The ROMP toolbox upgraded, Polymer 51 (2010) 2927−2946. https://doi.org/10.1016/j.polymer.2010.05.002.

[60] J.A. Love, J.P. Morgan, T.M. Trnka, R.H. Grubbs, A Practical and Highly Active Ruthenium-Based Catalyst that Effects the Cross Metathesis of Acrylonitrile, Angew. Chem., Int. Ed. 41 (2002) 4035−4037. https://doi.org/10.1002/1521-3773(20021104)41:21<4035::AID-ANIE4035>3.0.CO;2-I.

[61] T.L. Choi, R.H. Grubbs, Controlled living ring-opening-metathesis polymerization by a fast-initiating ruthenium catalyst, Angew. Chem. Int. Ed. 42 (2003) 1743−1746. https://doi.org/10.1002/anie.200250632.

[62] J.D. Rule, J.S. Moore, ROMP Reactivity of *endo*- and *exo*-Dicyclopentadiene, Macromolecules 35 (2002) 7878–7882. https://doi.org/10.1021/ma0209489.

[63] Y. Nishihara, Y. Inoue, Y. Nakayama, T. Shiono, K. Takagi, Comparative Reactivity of *Exo*- and *Endo*-Isomers in the Ru-Initiated Ring-Opening Metathesis Polymerization of Doubly Functionalized Norbornenes with Both Cyano and Ester Groups, Macromolecules 39 (2006) 7458–7460. https://doi.org/10.1021/ma061781c.

[64] D. Moatsou, C. F. Hansell, R. K. O'Reilly, Precision polymers: a kinetic approach for functional poly(norbornenes), Chem. Sci. 5 (2014) 2246–2250. https://doi.org/10.1039/C4SC00752B.

[65] T.P. Lin, A.B. Chang, H.Y. Chen, A.L. Liberman-Martin, C.M. Bates, M.J. Voegtle, C.A. Bauer, R.H. Grubbs, Control of Grafting Density and Distribution in Graft Polymers by Living Ring-Opening Metathesis Copolymerization, J. Am. Chem. Soc. 139 (2017) 3896−3903. https://doi.org/10.1021/jacs.7b00791.

[66] A.B. Chang, T.P. Lin, N.B. Thompson, S.X. Luo, A.L. Liberman-Martin, H.Y. Chen, B. Lee, R.H. Grubbs, Design, Synthesis, and Self-Assembly of Polymers with Tailored Graft Distributions, J. Am. Chem. Soc. 139 (2017) 17683−17693. https://doi.org/10.1021/jacs.7b10525.

[67] C. Nicolas, L. Fontaine, V. Montembault, Nitroxide radical-containing polynorbornenes by ring-opening metathesis polymerization as stabilizing agents for polyolefins, Polym. Chem. 10 (2019) 5487−5497. https://doi.org/10.1039/C9PY00769E.

[68] J.S. Fisk, R.A. Mosey, J.J. Tepe, The diverse chemistry of oxazol-5-(4*H*)-ones, Chem. Soc. Rev. 36 (2007) 1432–1440. https://doi.org/10.1039/B511113G.

[69] B. Couturaud, Z.H. Houston, G.J. Cowin, I. Prokes, J.C. Foster, K.J. Thurecht, R.K. O'Reilly, Supramolecular Fluorine Magnetic Resonance Spectroscopy Probe Polymer Based on Passerini Bifunctional Monomer, ACS Macro Lett. 8 (2019) 1479−1483. https://doi.org/10.1021/acsmacrolett.9b00626.

[70] A.C. Engler, X. Ke, S. Gao, J.M.W. Chan, D.J. Coady, R.J. Ono, R. Lubbers, A. Nelson, Y.Y. Yang, J.L. Hedrick, Hydrophilic Polycarbonates: Promising Degradable Alternatives to Poly(ethylene glycol)-Based Stealth Materials, Macromolecules 48 (2015) 1673–1678. https://doi.org/10.1021/acs.macromol.5b00156.

[71] C. Feng, X. Huang, Polymer Brushes: Efficient Synthesis and Applications, Acc. Chem. Res. 51 (2018) 2314−2323. https://doi.org/10.1021/acs.accounts.8b00307.

[72] J.M. Noy, Y. Li, W. Smolan, P.J. Roth, Azide–*para*-Fluoro Substitution on Polymers: Multipurpose Precursors for Efficient Sequential Postpolymerization Modification Macromolecules 52 (2019) 3083−3091. https://doi.org/10.1021/acs.macromol.9b00109.

[73] F. Kollinsky, K. Hubner, G. Markert, US Patent 3,598,790A (1970).

[74] H.W. Horn, G.O. Jones, D.S. Wei, K. Fukushima, J.M. Lecuyer, D.J. Coady, J.L. Hedrick, J.E. Rice, Mechanisms of Organocatalytic Amidation and Trans-Esterification of Aromatic Esters As a Model for the Depolymerization of Poly(ethylene) Terephthalate, J. Phys. Chem. A 116 (2012) 12389–12398. https://doi.org/10.1021/jp304212y.

[75] J. Demarteau, I. Olazabal, C. Jehanno, H. Sardon, Aminolytic upcycling of poly(ethylene terephthalate) wastes using a thermally-stable organocatalyst, Polym. Chem. 11 (2020) 4875–4882. https://doi.org/10.1039/d0py00067a.

[76] L. Yuan, Z. Wang, N.M. Trenor, C. Tang, Robust Amidation Transformation of Plant Oils into Fatty Derivatives for Sustainable Monomers and Polymers, Macromolecules 48 (2015) 1320–1328. https://doi.org/10.1021/acs.macromol.5b00091.

[77] L. Yuan, Z. Wang, N.M. Trenor, C. Tang, Amidation of triglycerides by amino alcohols and their impact on plant oil-derived polymers, Polym. Chem. 7 (2016) 2790–2798. https://doi.org/10.1039/ c6py00048g.

Graphical abstract